Supporting Information

Carbohydrate-Conjugated Hollow Oblate Mesoporous Silica Nanoparticles as Nanoantibiotics to Target Mycobacteria

*Nanjing Hao, Xuan Chen, Seaho Jeon, and Mingdi Yan**

Department of Chemistry, University of Massachusetts, Lowell, MA 01854, USA. E-mail: mingdi_yan@uml.edu; Fax: +1-978-934-3013; Tel: +1-978-934-3647

1. Materials

Cetyltrimethylammonium bromide (CTAB), dibenzyl ether, tetraethyl orthosilicate (TEOS), ammonium hydroxide (25%), ethanol (200-proof), D-(+)-mannose, D-(+)-trehalose, and isoniazid (INH) were purchased from Sigma-Aldrich. Water used was from a Milli-Q ultrapure water purification system. All chemicals were used as received without any further purification.

Middlebrook 7H9 broth with oleic acid-albumin-dextrose-catalase (OADC) enrichment was prepared by mixing Middlebrook 7H9 (4.7 g, BD bioscience), glycerol (2.0 mL, Acros Organics), and water (900 mL). After sterilization by autoclaving (Tuttnauer EZ 10, Hauppauge, NY), OADC (100 mL, BD bioscience) and Tween 80 (0.05%, Sigma) were added.

2. Synthesis of oblate mesoporous silica nanoparticles (OMSNs)

CTAB (0.45 g) was dissolved in water (148 mL), and dibenzyl ether (2 mL) was added. Next, $NH_3 \cdot H_2O$ (25%, 2.5 mL) was added with stirring for 10 min at room temperature. TEOS (4 mL) was finally added with stirring for another 5 h. After centrifugation followed by washing

three times with deionized water, the resulting solid was dried at 80 °C overnight. The CTAB template was removed by heating in static air up to 600 °C at a rate of 1 °C/min.

3. Synthesis of hollow oblate mesoporous silica nanoparticles (HOMSNs)

The freshly prepared OMSNs (150 mg) were dispersed in deionized water (30 mL) by sonication. After addition of ammonia (4 mL) and then stirring for 1 h at room temperature, the mixture was transferred into a sealed, Teflon-lined autoclave and heated at 120 °C for 2 h. The autoclave was then cooled to room temperature. The product was collected and washed with deionized water three times by centrifugation, then dried in a vacuum oven at 80 °C overnight.

4. Synthesis of PFPA-functionalized HOMSNs

N-(3-Trimethoxysilylpropyl)-4-azido-2,3,5,6-tetrafluorobenzamide (PFPA-silane) was synthesized following a previously reported procedure.[1] HOMSNs were functionalized by PFPA following the procedure shown in Figure S1. HOMSNs (100 mg) was dispersed in toluene (20 mL), and PFPA-silane (50 mg) was added into this suspension. The mixture was stirred overnight at 60 °C. The resulting particles were collected by centrifugation and washing three times with acetone.

5. Conjugation of carbohydrate to PFPA-functionalized HOMSNs

Trehalose or mannose was conjugated to PFPA-functionalized HOMSNs following previously developed protocols (Figure S1).[1] A solution of PFPA-functionalized HOMSNs in acetone (2 mg/mL, 1 mL) was placed in a flat-bottom glass dish, and an aqueous solution of trehalose or mannose (10 mg/mL, 0.2 mL) was added. A 280 nm long-pass optical filter (WG-280, Schott Glass) was placed on top of the glass dish, and the mixture was irradiated with a 450 W medium-pressure Hg lamp (Hanovia, 3.2 mW/cm^2 measured by a 254 nm

sensor) for 30 min under vigorous stirring. The resulting trehalose-modified particles (HOMSNs-Tre) and mannose-modified particles (HOMSNs-Man) were purified by centrifugation and redispersion in Milli-Q water followed by membrane dialysis for 24 hours.

6. Loading and releasing of isoniazid (INH)

To load INH, particles (HOMSNs, HOMSNs-Tre, and HOMSNs-Man (30 mg) were suspended in an aqueous solution of INH (30 mg/mL, 1 mL). The mixture was stirred for 48 h at room temperature, and the drug-loaded nanoparticles were collected by centrifugation and careful washing with water twice to remove INH adsorbed on the particle surface. All supernatants were collected and measured by UV-vis spectroscopy at 260 nm to determine the amount of INH that was not loaded in the nanoparticles, using a standard calibration curve constructed by measuring the absorbance of INH solutions at varying concentrations (Figure S16). The amount of INH loaded in the nanoparticles was then computed by subtracting the unloaded from the initially added.

For drug release, the INH-loaded samples (2 mg) were added to PBS buffer (pH 6.6), and the supernatant was collected at given time intervals. The supernatant was measured by UV-vis spectroscopy at 260 nm to determine the concentration of INH released.

7. Antibacteria assays

Mycobacteria (*M. smegmatis* strain mc^2 651) were inoculated overnight in enriched Middlebrook 7H9 broth at 37 °C while shaking at 200 rpm until an optical density (OD_{650}) of 0.3 (ca. 10^8 CFU/mL) was reached. An aliquot of this bacteria suspension (1 mL) was taken and was serially diluted 100 folds in Middlebrook 7H9 broth. From this dilution, 100 μL aliquots were incubated for 48 h with different concentrations of HOMSNs, HOMSNs-INH, HOMSNs-Tre, HOMSNs-Tre-INH, HOMSNs-Man, HOMSNs-Man-INH, and free INH at 37 °C in a humidified incubator shaker (250 rpm). Colony counting was obtained from the

microdiluted plate. An aliquot of 10 μL from each well of the bacterial suspension was taken, and serially diluted in Middlebrook 7H9 broth. From the dilution, 20 μL was spread out on Middlebrook 7H10 agar plates, and the plates were incubated at 37 °C for 72 h. Colonies were counted and reported as log CFU/mL.

8. Inhibition zones test

A previously reported procedure was adapted.[2] Briefly, the bacterial suspension (100 μL, 10^6 CFU/mL) was uniformly spread on Middlebrook 7H10 agar Petri dish, and incubated for 10 minutes at room temperature. Sterilized paper disks of 7 mm diameter were impregnated with INH or INH-loaded mesoporous silica samples (equivalent to 5 mg drug). The disk was then placed on the Petri dishes close to the agar surface. Bacteria were then allowed to grow for 24, 36, or 48 h at 37 °C. The diameter of the bacteria-free zone surrounding the disk was measured. The experiment was performed with three independent repetitions.

9. Interactions of HOMSNs with bacteria

Mycobacteria (*M. smegmatis* strain mc^2 651) were inoculated overnight in the Middlebrook 7H9 broth at 37 °C and 200 rpm until an OD_{650} of 0.3 was attained. The bacteria cells were then harvested, centrifuged at 2000 rpm, and re-dispersed in broth medium. HOMSNs-INH, HOMSNs-Tre-INH, and HOMSNs-Man-INH (with equivalent INH drug concentration of 100 μg/mL) were added to an aliquot of bacteria (ca. 10^6 CFU), and the mixture was incubated at 37 °C for different time periods (0, 0.5, 1, 2, 4, and 8 h) while shaking at 150 rpm. The mixture was then centrifuged and washed for several times, and each time the supernatant containing free nanoparticles was discarded. A drop of final bacteria cell suspension was placed onto a Cu grid followed by vacuum drying overnight for TEM imaging.

10. Characterization

The morphology of the oblate mesoporous silica nanoparticles was examined by TEM using a Phillips EM-400 TEM microscope operating at an accelerating voltage of 100 kV. Scanning electron microscopy (SEM) images were obtained on a JEOL JSM 7401F FE-SEM instrument operated at 15 kV. Samples were sputtered with Au prior to characterization. Nitrogen adsorption–desorption measurements were carried out using a Quantachrome Autosorb-3B surface area analyzer at −196 °C. The specific surface area was calculated by the Brunauer-Emmett-Teller (BET) method. Pore-size distributions were estimated using the Barrett–Joyner–Halenda (BJH) method. Pore volumes were determined from the amounts of N_2 adsorbed at the single point of P/P_0 =0.98. The infrared spectra were recorded on a Nicolet 6700 FT-IR spectrometer from Thermo Scientific Corporation. Thermogravimetric analysis (TGA) was carried out on Q50 (TA Instrument, DE); samples were heated from room temperature to 1000 °C at a heating rate of 20 °C/min.

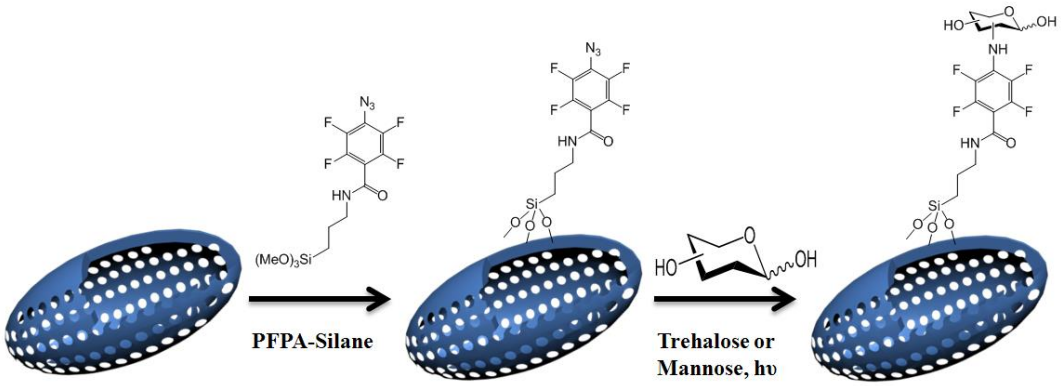

Figure S1. Synthesis of carbohydrate-functionalized HOMSNs.

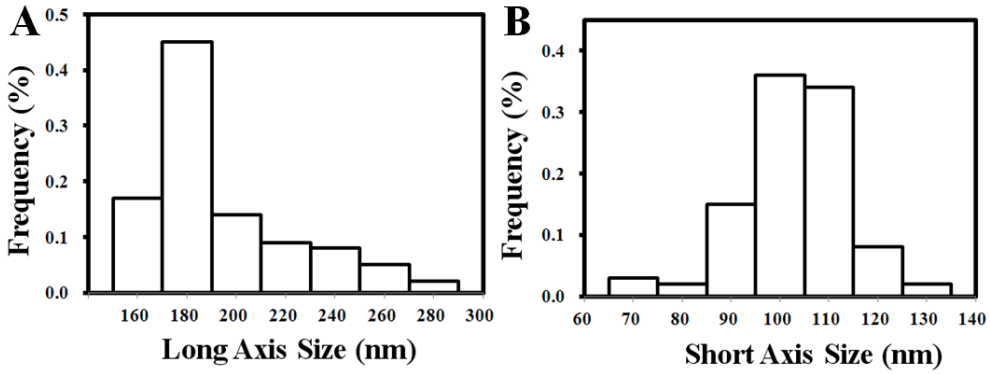

Figure S2. Statistical long axis (A) and short axis (B) size distribution of OMSNs from 200 particles in the TEM images.

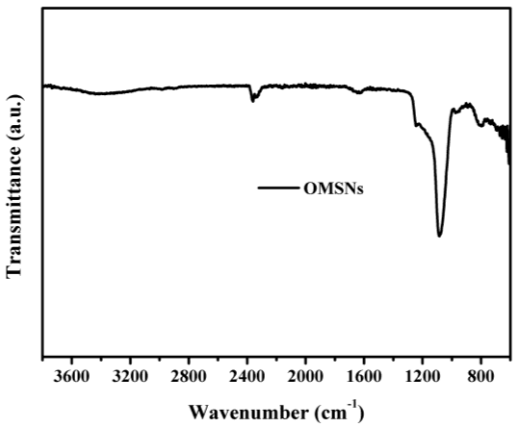

Figure S3. FTIR spectrum of OMSNs after removing CTAB by calcination.

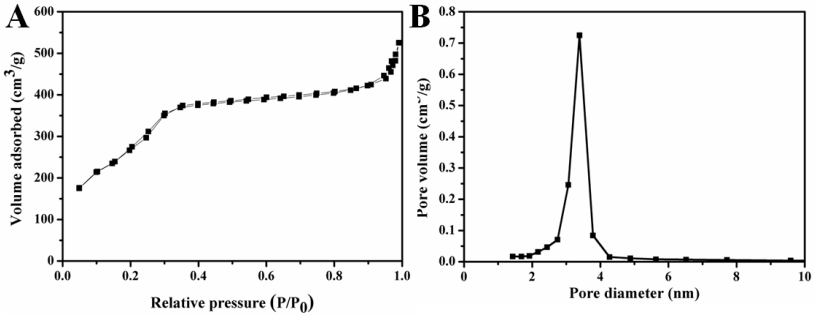

Figure S4. (A) N_2 adsorption-desorption isotherm of OMSNs. (B) The corresponding pore size distribution plot by the BJH method.

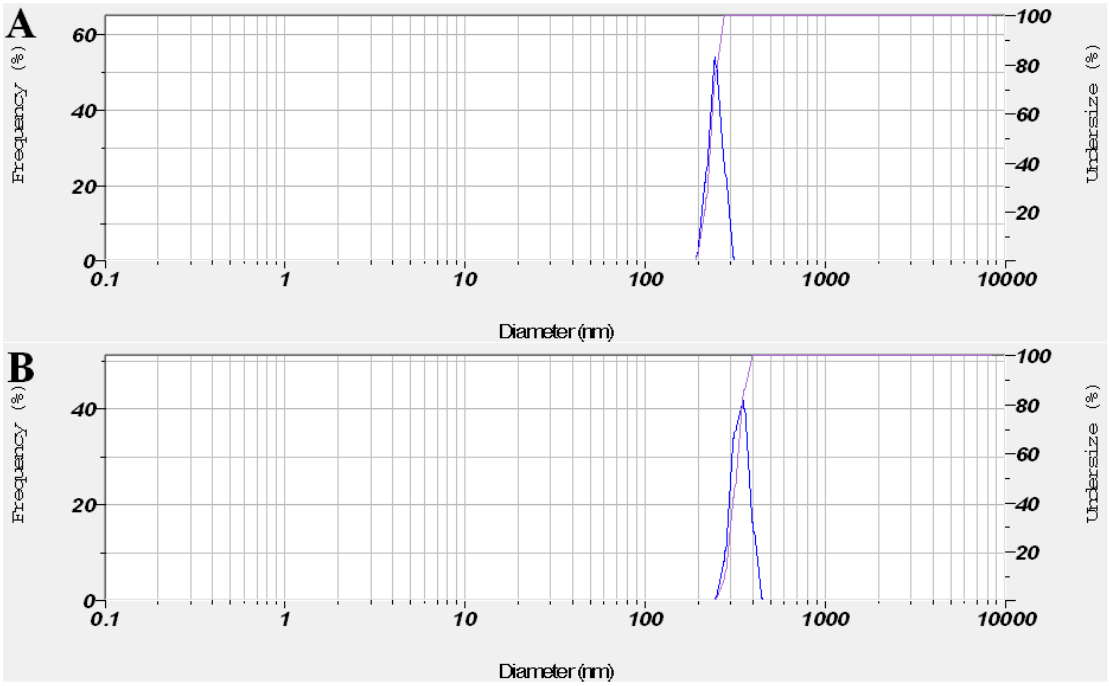

Figure S5. DLS results of OMSNs (A) and HOMSNs (B) that shows the average hydrodynamic diameter of 234.1 and 322.3 nm, respectively.

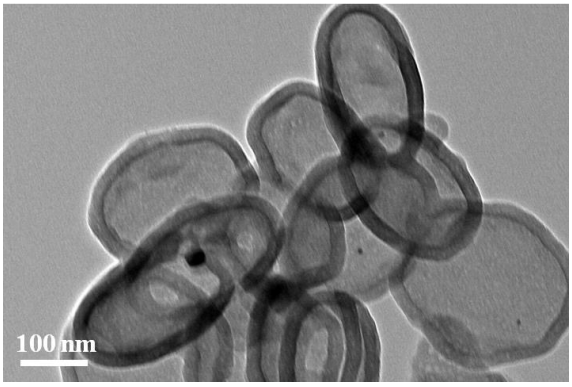

Figure S6. TEM image of HOMSNs after treated in PBS buffer for 48 h at 37 °C.

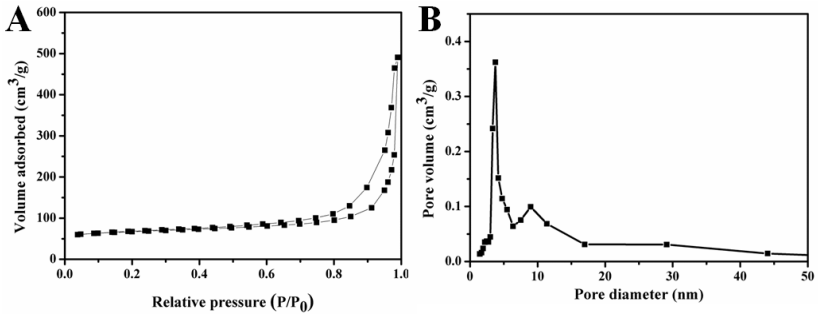

Figure S7. (A) N_2 adsorption-desorption isotherm of HOMSNs. (B) The corresponding adsorption pore size distribution plot by the BJH method.

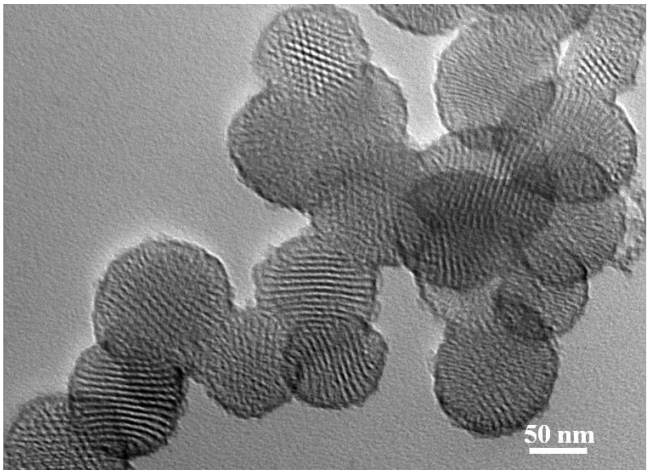

Figure S8. TEM image of particles prepared by following the same protocol as that of OMSNs except changing the amount of dibenzyl ether from 2 mL to 6 mL. The resulting particles had an average pore size of 5.8 nm instead of 3.3 nm, and took a spherical instead of oblate ellipsoidal morphology.

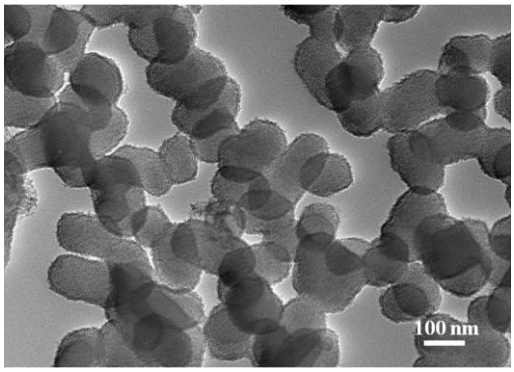

Figure S9. TEM image of particles prepared by following the same protocol as that of OMSNs except without the addition of dibenzyl ether. The particles exhibited rod-shape morphology.

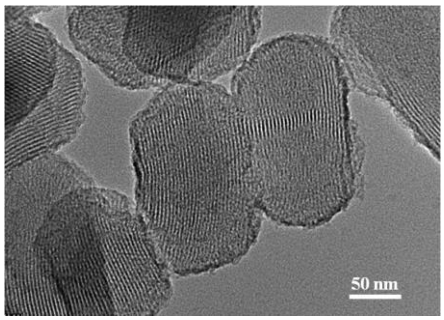

Figure S10. TEM image of particles prepared by following the same protocol as that of OMSNs except changing the amount of CTAB from 0.45 g to 0.6 g. The resulting particles exhibited rod-shape morphology with pore channels running along the long axis.

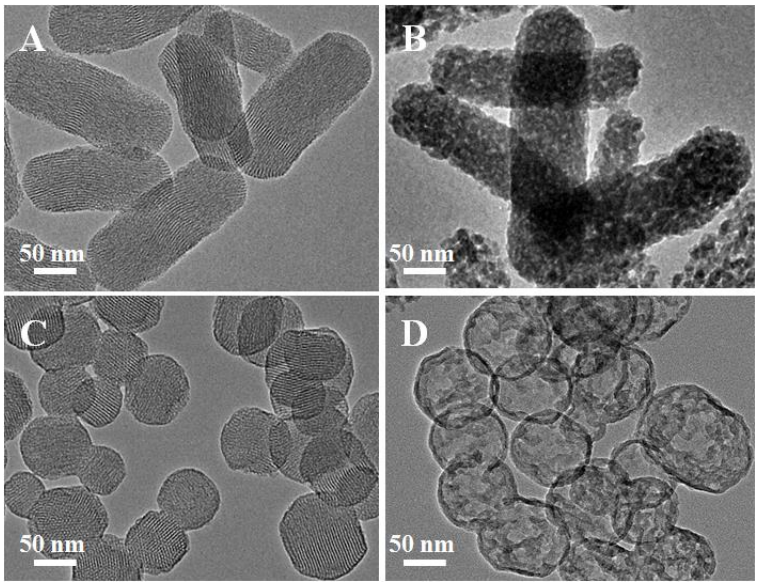

Figure S11. TEM images of rod- and sphere-shaped mesoporous silica nanoparticles before (A and C) and after (B and D) treating with ammonia under hydrothermal conditions (following the same protocol as that of OMSNs, *i.e.*, 150 mg nanoparticles with 4 mL ammonia and 30 mL water at 120 °C for 2 h in an autoclave). The results showed that the evolution of hollow nanostructure was affected by the direction and density of pore channels. Rod-shaped nanoparticles with pore channels running along the long axis (A) could not be converted to hollow nanostructures (B), likely due to fewer pore channels compared to those running parallel to the short axis. Spherical nanoparticles with regular pore channels (C) could evolve into hollow nanospheres but with thinner shells (D).

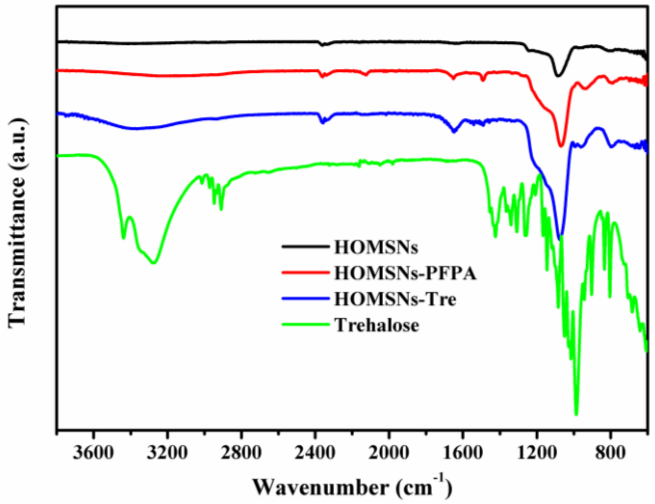

Figure S12. FTIR spectra of HOMSNs, HOMSNs-PFPA, HOMSNs-Tre, and trehalose.

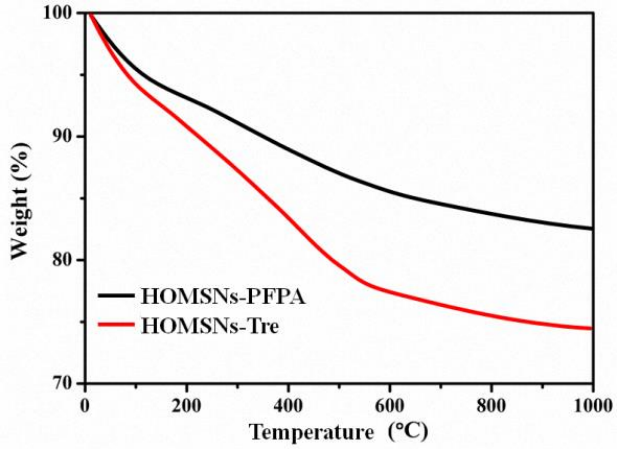

Figure S13. TGA decomposition plots of HOMSNs-PFPA (weight loss ~17.5%) and HOMSNs-Tre (weight loss ~25.6%).

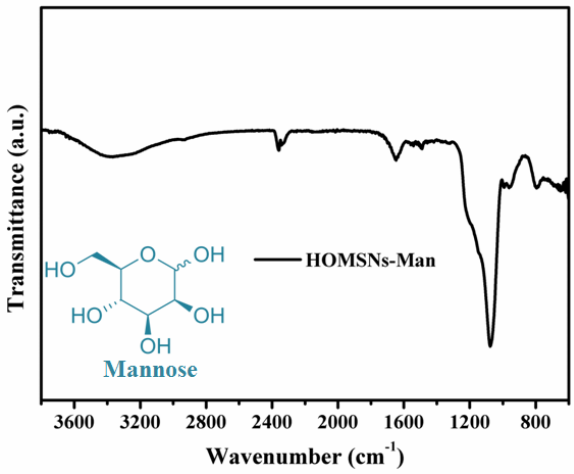

Figure S14. FTIR spectrum of HOMSNs-Man. Inset is the structure of mannose.

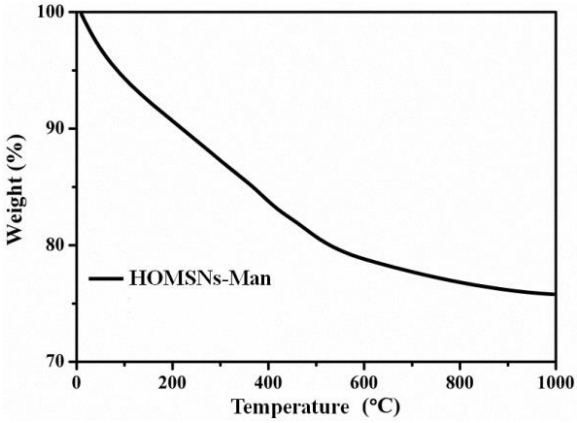

Figure S15. TGA decomposition plot of HOMSNs-Man (weight loss ~24.8%).

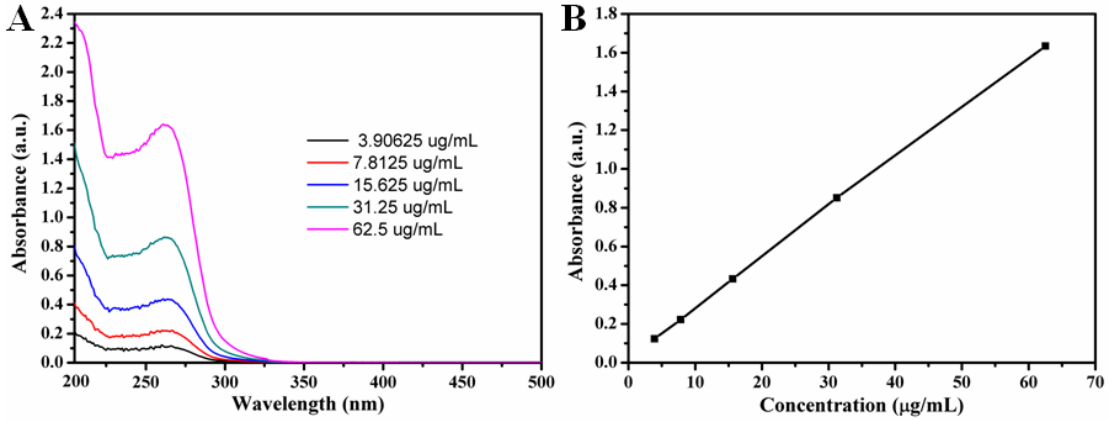

Figure S16. (A) UV-vis spectra of different concentrations of INH in water. (B) Standard calibration curve of INH in water at 260 nm (R^2=0.9996).

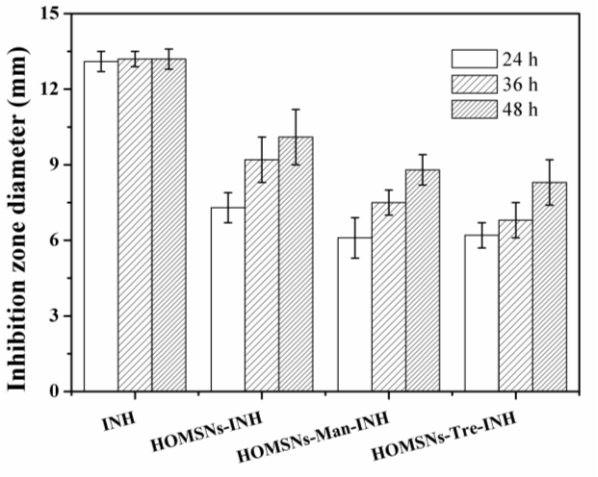

Figure S17. Inhibition zones of INH, HOMSNs-INH, HOMSNs-Man-INH, and HOMSNs-Tre-INH against *M. smegmatis* strain mc^2 651 for 24, 36, and 48 h.

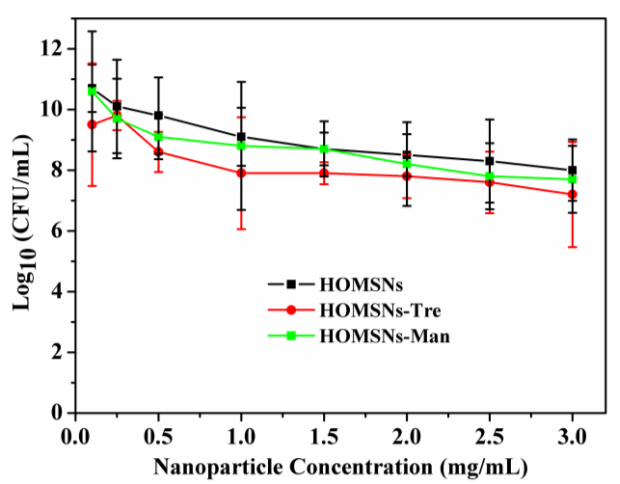

Figure S18. Antibacterial efficacy of HOMSNs, HOMSNs-Tre, and HOMSNs-Man at the concentration range from 0.1 to 3 mg/mL for 48 h.

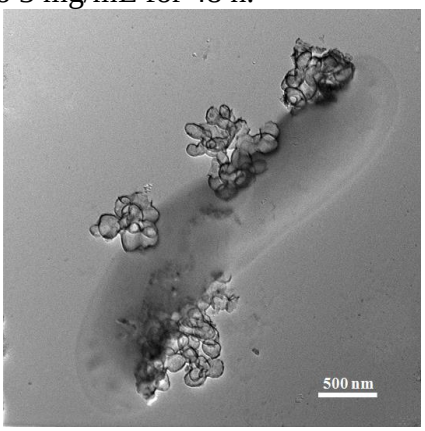

Figure S19. TEM image of mycobacteria treated with HOMSNs-INH for 8 h.

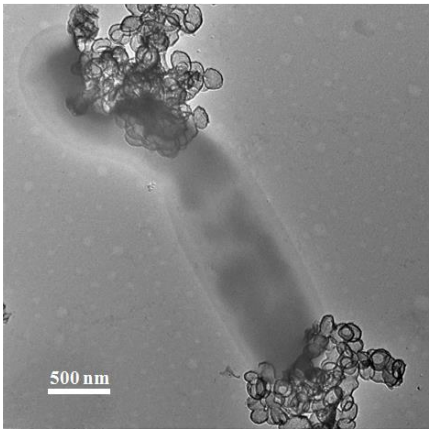

Figure S20. TEM image of mycobacteria treated with HOMSNs-Man-INH for 8 h.

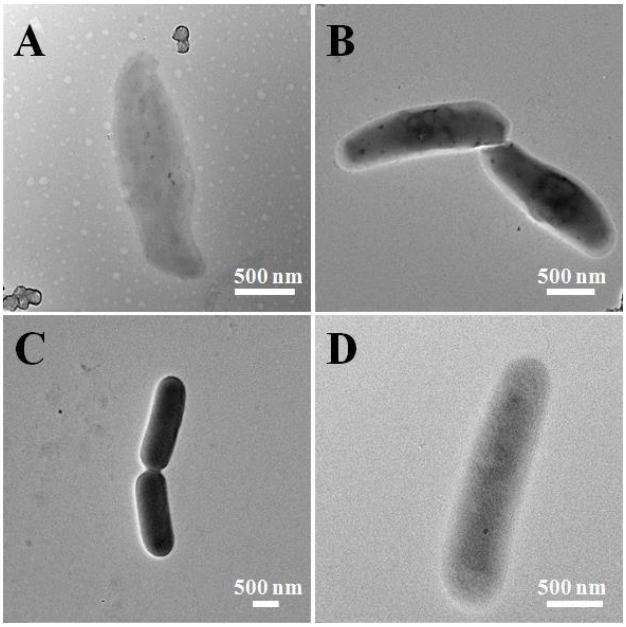

Figure S21. (A)-(B) TEM images of *E. coli* ORN 178 (A) and *E. coli* ORN 208 (B) treated with HOMSNs-Tre-INH for 8 h. (C)-(D) TEM images of *E. coli* ORN 178 treated with HOMSNs (C) and HOMSNs-INH (D) for 8 h. The *E. coli* bacteria were maintained in Muller Hinton Broth (BD bioscience).

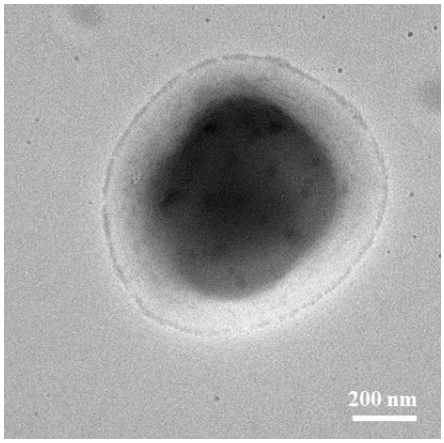

Figure S22. TEM images of *Staphylococcus epidermidis* treated with HOMSNs-Tre-INH for 8 h. The *Staphylococcus epidermidis* bacteria were maintained in Tryptic Soy Broth (BD bioscience).

Reference

[1] a) S. A. Al-Baraineh; R. Luginbuehl; M. Textor; M. Yan, *Langmuir* **2009**, *25*, 7432; b) X. Wang; E. Matei; L. Deng; O. Ramström; A. Gronenborn; M. Yan, *Chem. Commun.* **2011**, *47*, 8620; c) X. Wang; O. Ramström; M. Yan, *Analyst* **2011**, *136*, 4174; d) Q. Tong; X. Wang; H. Wang; T. Kubo; M. Yan, *Anal. Chem.* **2012**, *84*, 3049; e) C. Xu, K. M. A. Uddin, X. Shen, S. Jayawadena, M. Yan, L. Ye, *ACS Appl. Mater. Interface* **2013**, *5*, 5208.

[2] a) C. M. Hao, Y. Z. Cui, P. F. Yang, H. Y. Zhang, D. J. Mao, X. Cui, J. Y. Li, *Colloids Surf. B* **2015**, *128*, 528; b) A. H. El-masry, H. H. Fahmy, S. H. A. Abdelwahed, *Molecules* **2000**, *5*, 1429; c) G. S. Alvarez, C. Hélary, A. M. Mebert, X. L. Wang, T. Coradin, M. F. Desimone, *J. Mater. Chem. B*, **2014**, ***2***, 4660.